Biosensors and Bioelectronics 26 (2011) 3602–3607

Contents lists available at ScienceDirect

Biosensors and Bioelectronics

journal homepage: www.elsevier.com/locate/bios

A novel hydrogen peroxide biosensor based on the immobilization of hemoglobin on three-dimensionally ordered macroporous (3DOM) gold-nanoparticle-doped titanium dioxide (GTD) film

Nannan Wei[a,b,c], Xin Xin[a,b,c], Jiangyan Du[a,b,c,*], Jianlin Li[d]

[a] College of Chemistry and Materials Science, Nanjing Normal University, Nanjing 210097, China
[b] Jiangsu Key Laboratory of New Power Batteries, Nanjing 210097, China
[c] Jiangsu Key Laboratory of Biofunctional Materials, Nanjing 210097, China
[d] Department of Food Science and Nutrition, Nanjing Normal University, Nanjing 210097, China

ARTICLE INFO

Article history:
Received 30 November 2010
Received in revised form 24 January 2011
Accepted 9 February 2011
Available online 16 February 2011

Keywords:
Hemoglobin
Gold-nanoparticle-doped
Titanium dioxide
Hydrogen peroxide
Electrocatalysis

ABSTRACT

The three-dimensionally ordered macroporous gold-nanoparticle-doped titanium dioxide (3DOM GTD) film was modified on the indium-tin oxide (ITO) electrode surface. Hemoglobin (Hb) has been successfully immobilized on the 3DOM GTD film and the fabrication process was characterized by Raman and UV–vis spectra. The results indicated that the Hb immobilized on the film retained its biological activity and the secondary structure of Hb was not destroyed. The direct electrochemistry and electrocatalysis of Hb immobilized on this film have been investigated. The Hb/3DOM GTD/ITO electrode exhibited two couples of redox peaks corresponding to the Hb intercalated in the mesopores and adsorbed on the external surface of the film with the formal potential of −0.20 and −0.48 V in 0.1 M PBS (pH7.0), respectively. The Hb/3DOM GTD/ITO electrode exhibits an excellent eletrocatalytic activity, a wide linear range for H_2O_2 from 5.0 μM to 1.0 mM with a limit of detection of 0.6 μM, high sensitivity (144.5 μA mM^{-1}), good stability and reproducibility. Compared with the TiO_2 nanoneedles modified electrode, the GTD modified electrode has higher sensitivity and response peak current. The 3DOM GTD provided a good matrix for bioactive molecules immobilization, suggesting it has the potential use in the fields of H_2O_2 biosensors.

1. Introduction

The sensitive and accurate detection of hydrogen peroxide (H_2O_2) is becoming of practical importance in the pharmaceutical, environmental, biological, clinical and industrial settings fields (Bartlett et al., 1998; Chen et al., 2006; Yu and Ju, 2003). Electrochemical methods for H_2O_2 detection have been demonstrated to be simple, rapid, and inexpensive methods and extensively employed for the design of H_2O_2 biosensors. However, the miniaturization trend of electrochemical biosensors makes the design and utilization of them have been of high interest.

The direct electrochemistry of enzymes and proteins has attracted considerable attention because it provides fundamental knowledge of redox behavior of enzymes or proteins in a biological system and is a more effective way of fabricating biosensors, bioreactors, and biomedical devices than using mediators (Armstrong and Wilson, 2000; Hamachi et al., 1997; Armstrong et al., 1988; Szpakowska et al., 2009). Although enzymes or proteins electron-transfer are quite fast in biological systems, they exhibit rather slow rate of heterogeneous electron-transfer at conventional electrodes because of the deep burying of the electroactive center of enzymes or proteins, the adsorptive denaturation and the unfavorable orientations on the electrodes. Therefore, it is still a challenge to achieve direct electrochemistry of enzymes and proteins.

In order to improve the electrochemical properties of enzymes or proteins and retain their bioactivities, multiporous structure materials have been used to prepare the modified electrode for their high active surface area and increase significantly detection signals (Alwarappan et al., 2010; Teng et al., 2009). Among the multiporous structures, three-dimensionally ordered macroporous (3DOM) (>50 nm) modified electrodes materials have recently received extensive attention (Lu and Eychmueller, 2008; Song et al., 2005; Szamocki et al., 2006, 2007). These 3DOM modified electrodes can ensure the accessibility of reactants to the active surface sites of electrodes, increasing both the mass transport of reactant and mass-normalized activity. These open, interconnected and periodic 3DOM structures provide a high stability, an increase of up to 2 orders of magnitude active surface area, more than one order of magnitude signal compared to that on a flat electrode. Therefore, the electrochemical detection with the 3DOM modi-

* Corresponding author at: College of Chemistry and Materials Science, Nanjing Normal University, Nanjing 210097, China. Tel.: +86 25 85891767; fax: +86 25 85891767.
E-mail address: dujiangyan@njnu.edu.cn (J. Du).

0956-5663/$ – see front matter © 2011 Elsevier B.V. All rights reserved.
doi:10.1016/j.bios.2011.02.010

fied multiporous electrodes have become apparent and fascinating in the electrochemistry field. Among the modified electrodes, the 3DOM TiO_2 film is of particular interest for its optical transparency, good biocompatibility, environmental safety and relatively good electrical conductivity. Since the first report claiming the synthesis of 3DOM TiO_2 photonic crystals, 3DOM TiO_2 films have been used in rechargeable lithium ion batteries (Bing et al., 2006), solar cells (Huisman et al., 2005), photocatalysts (Environ, 2007) and electrochemical biosensor (Zhang et al., 2004). Recently, 3DOM TiO_2 film modified electrodes have been reported for immobilization of HRP (Zhu et al., 2009) and glucose oxidase (Cao et al., 2008a,b). In our previous work, we fabricated a new 3DOM gold-nanoparticle-doped titanium dioxide (GTD) photonic crystals modified electrode by the colloidal crystal template technique and developed a new HRP-based H_2O_2 biosensor using the 3DOM GTD/ITO electrode (Li et al., 2009a,b). 3DOM gold nanoparticles/TiO_2 composite architecture exhibited to promote the direct electron transfer of the immobilized enzymes and further enhance the sensitivity of the designed H_2O_2 electrochemical biosensor.

Hemoglobin (Hb) is a desirable model molecule for the study of electron transfer reactions of heme enzymes (Ma et al., 2007; Tang et al., 2008; Wei et al., 2009; Wu and Hu, 2007) and can be used as a substitute of horseradish peroxidase (HRP) to catalyze the reduction of H_2O_2 (Feng et al., 2005; Li et al., 2009a,b; You et al., 2009). In this work, Hb was successfully immobilized on the 3DOM GTD film and Hb-based H_2O_2 electrochemical biosensor was fabricated. The fabrication process was characterized by Raman spectroscopy, UV–vis spectroscopy. This is the first report on the 3DOM GTD/ITO electrode for biosensor for direct electrochemistry of Hb. The results indicated that the secondary structure of Hb immobilized on the film was not destroyed and retained its biological activity. The amperometric response of the immobilized Hb had a good linear relation with the concentration of H_2O_2 and the quantitative relationship between the responsive current intensity and H_2O_2 concentration was established. The electrode modified with Hb/3DOM GTD film has higher stability and eletrocatalytic activity toward the reduction of H_2O_2 compared with the electrode modified with the gold-nanoparticle-doped titanium dioxide nanoneedles (GTDNs) film. The developed biosensor provides a new matrix for study of direct electrochemistry of enzymes and proteins and detection of H_2O_2 on low conductivity electrode biosensor.

2. Experimental

2.1. Materials

Bovine hemoglobin (Hb, MW 64,500, EC 1.11.17, RZ > 3.0, A > 300 units/mg) purchased from Sigma Chemical Co. was used without further purification. Titanium (IV) butoxide, H_2O_2 (30%) and ethanol absolute were purchased from Chemical Reagents Co., Ltd. of China. Triethanolamine (TEA), $HAuCl_4$ were purchased from the Nanjing Sunshine Biotechnology Ltd., China. TiO_2 nanoneedles were synthesized in Southeast University, China. The water was Mili-Q water at 18' MΩ. All other chemicals were of analytical grade and were used without further purification. ITO glasses (<20 Ω/cm^2) were purchased from Wuxi Kang Li Electron Industry Co., Ltd of China. The diameter 290 ± 15 nm polystyrene (PS) microspheres were synthesized in our laboratory.

2.2. Apparatus

The UV–vis spectra were recorded using a Lambda 17 UV spectrophotometer (Perkin–Elmer, USA) with a cuvette of 1 cm path length. The Raman spectra were obtained on a Labram 800 UV Raman spectrometer at ambient temperatures using 514.5 nm excitation and a spectral slit width of 600g cm^{-1}. The scanning electron microscopy (SEM) images were obtained with a Quanta-200 microscope (FEI, Holand).

Cyclic voltammetric (CV) and amperometric response measurements were carried out on a CHI760 electrochemical workstation (CHI Instruments, USA) employing a conventional three-electrode cell. The saturated calomel electrode (SCE) and a platinum electrode were used as the reference electrode and counter electrode, respectively. A Hb/3DOM GTD/ITO electrode was used as the working electrode.

2.3. Substrate preparation

Gold colloids were prepared according to the method reported by Doron et al. (1995). The products were stored in brown glass bottles at 4 °C. GTD sol–gel solution was synthesized according to our previous work (Li et al., 2009a,b). The preparation of 3DOM GTD photonic crystals was performed by the colloidal crystal template method. The surface morphology of the 3DOM GTD photonic crystals was characterized by SEM shown as Fig. 1A. The SEM image shows that the film is face-centered cubic ordered hexagonal network structure and the gold nanoparticles are introduced within the framework. The hexagonal networks stack layer-by-layer forming a 3DOM periodical structure with the interpenetrated pores.

Prior to modification, ITO glasses were cleaned ultrasonically 3 times with deionized water. The cleaned ITO substrates were immersed into 0.2% (v/v_0) colloidal suspension of PS microspheres for 48 h at the room temperature. The fix of PS template on ITO substrates, the infiltration of GTD colloids solution into the interspaces of PS opal template and the removing of the template were performed (Li et al., 2009a,b). The ITO substrates modified with GTD photonic crystals were cut at 1 cm × 1 cm area.

The TiO_2 nanoneedles were dispersed in deionized water with the aid of ultrasonic agitation for 2 h. Then TiO_2 nanoneedles were mixed with 1% Au colloid solution and ultrasonic agitation for 1 h. The suspension was adjust to pH = 6 and centrifugated at 1.1×10^4 *g* for 15 min. During the process, the gold-nanoparticles would be absorbed on the surface of the TiO_2 nanoneedles forming gold-nanoparticle-doped TiO_2 nanoneedles adducts (GTDNs). The surface morphology of the GTDNs adducts was shown as Fig. 1B. The GTDNs/ITO electrode was fabricated by casting a sol of GTDNs on the surface of treated ITO electrode through the dip-coating method. Then the GTDNs/ITO electrode was sinteringed in the oven at 500 °C for 1 h. The ITO substrates modified with the GTDNs film were also cut at 1 cm × 1 cm area.

2.4. Hb immobilization

For preparation of the Hb electrode, the 3DOM GTD/ITO electrode was cleaned 2 times with ethanol absolute and immersed in 0.1 M pH 7.0 phosphate buffer solution (PBS) containing 5 mg/mL Hb at 4 °C for 24 h. Before electrochemical experiments, the electrode was rinsed thoroughly with doubly distilled water to remove unbound Hb and kept in PBS at 4 °C when not in use.

2.5. Electrochemical detection of H_2O_2

Cyclic voltammetric (CV) and amperometric response measurements were performed in a 10 mL electrochemical cell by a conventional three-electrode cell. A Hb/3DOM GTD/ITO electrode, SCE and platinum electrode were used as the working electrode, reference electrode and counter electrode, respectively. Prior to experiments, high-purity nitrogen was purged into solution for at least 15 min, and a continuous flow of the gas was kept over the solution during the experiments to protect the solution from

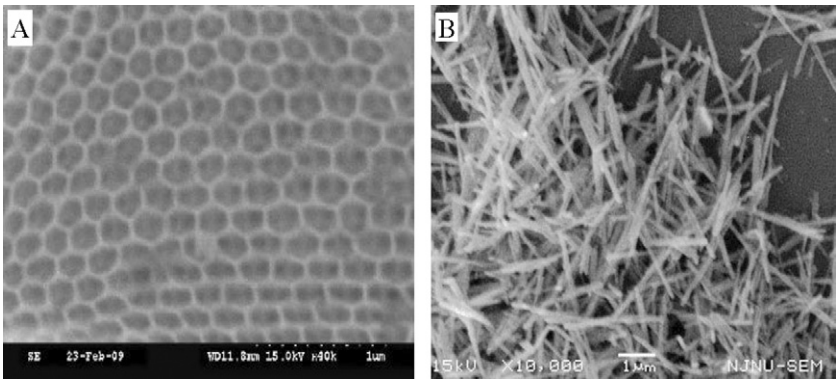

Fig. 1. The SEM of the 3DOM GTD flim (A) and the GTDNs film (B). The GTD photonic crystal films were obtained by infiltration 4 times with the 1:1 ethanol absolute dilution of GTD solution. The GTDNs films were obtained by mixing TiO_2 nanoneedles with 1% Au colloid solution and ultrasonic agitation for 1 h.

oxygen. Aliquots of a standard solution of H_2O_2 were successively added to the cell. All experiments were performed at the room temperature ($20 \pm 1\,^{\circ}C$).

3. Results and discussion

3.1. Spectroscopic characterization of Hb in the 3DOM GTD/ITO electrode

Raman spectroscopy was used to characterize the immobilize of Hb. Fig. 2 shows typical Raman spectra of 3DOM GTD (a), Hb-3DOM GTD (b) and Hb (not adsorbed) (c). Hb has three characteristic Raman peaks at 1593, 1370 and 1232 cm^{-1}, respectively (Fig. 2c). These characteristic peaks were also observed on the Raman spectrum of Hb-3DOM GTD film (Fig. 2b) and they did not appear on the Raman spectrum of 3DOM GTD film (Fig. 2a). These results suggest that Hb was effectively adsorbed on the surface of 3DOM GTD film.

The assembly of Hb on the surface of 3DOM GTD film was also verified by the results of UV–vis spectra as shown in supplementary material Figure 1. UV–vis spectrum of 3DOM GTD film showed a smooth curve. UV–vis spectrum of free Hb (not adsorbed) showed a adsorption peak at 404 nm which is the characteristic Soret absorption of Hb (Gu et al., 2001). This peak also appeared on the UV–vis spectrum of Hb-3DOM GTD. Furthermore, it showed that the position of absorption peak of Hb in Hb-3DOM GTD film was almost the same as that of free Hb, suggesting that the Hb immobilized on 3DOM GTD film still maintained its native structure (Nassar et al., 1995a).

3.2. Direct electron transfer of Hb in the 3DOM GTD/ITO electrode

In order to study the direct electron transfer of Hb in the 3DOM GTD/ITO electrode, cyclic voltammetric (CV) of 3DOM GTD/ITO and Hb/3DOM GTD/ITO electrode in 0.1 M PBS (pH 7.0) containing 0.1 M NaCl were studied over a potential range from −0.7 V to 0.2 V at scan rate of 100 mV^{-1}/s. As shown in Fig. 3, no signal of 3DOM GTD/ITO electrode was observed in the absence of Hb (Fig. 3a). In contrast, Hb/3DOM GTD/ITO electrode showed two couples of well-defined redox peaks which appeared at −0.43 V and −0.52 V for the first couple and −0.11 V and −0.30 V for another couple, respectively (Fig. 3b). The formal potentials $E^{0'}$ were −0.48 V and −0.20 V, respectively. The two couples of redox peaks come from the two states of the immobilized Hb, which occurring at lower potential were assigned to the redox of Hb intercalated in the mesopores, and another couple of redox peaks resulted from the redox of the Hb adsorbed on the external surface of the mesoporous structure by physical adsorption. Similar results were also reported in the studies of immobilized cytochrome c and HRP on nanoporous TiO_2 films (Liu and Chen, 2005; Topoglidis et al., 2001a,b; Dai et al., 2005). Our fabricated macroporous structure with 260 nm diameter is large enough to allow infiltration of Hb into the modified electrode. Therefore, Hb can be adsorbed not only on the exter-

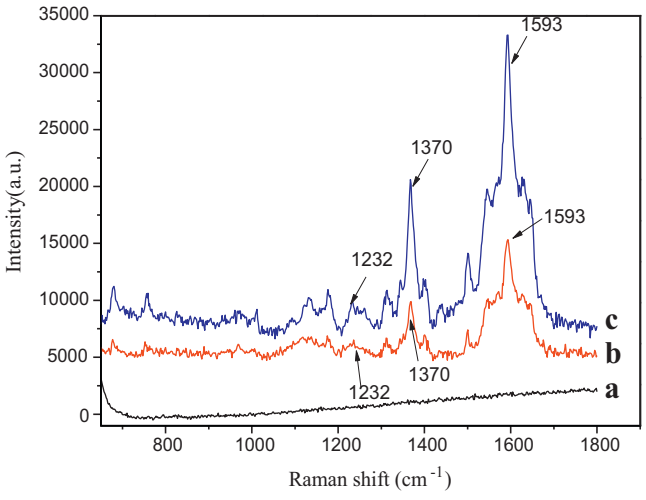

Fig. 2. Raman spectra of 3DOM GTD (a), Hb-3DOM GTD (b) and Hb (not adsorbed) (c). The Raman spectra were obtained at ambient temperatures using 514.5 nm excitation and a spectral slit width of 600 g cm^{-1}.

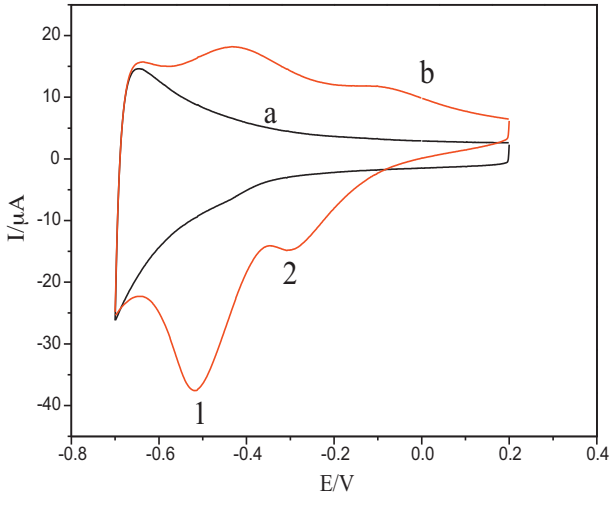

Fig. 3. CVs of the modified electrodes in 0.1 M PBS (pH 7.0) at 100 mV/s scan rate. (a) 3DOM GTD/ITO electrode, (b) Hb/3DOM GTD/ITO electrode. The SCE and Pt electrode were used as the reference electrode and counter electrode, respectively.

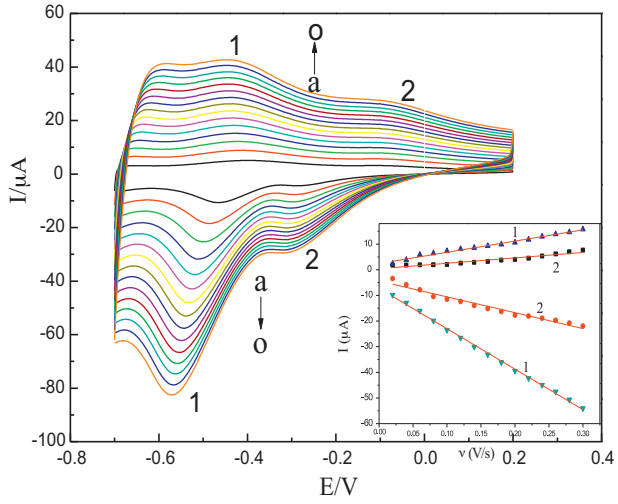

Fig. 4. The influence of scan rates on the response of Hb/3DOM GTD/ITO electrode in 0.1 M PBS (pH 7.0). Inset shows the relationship between the two couples of redox peak currents and scan rates.

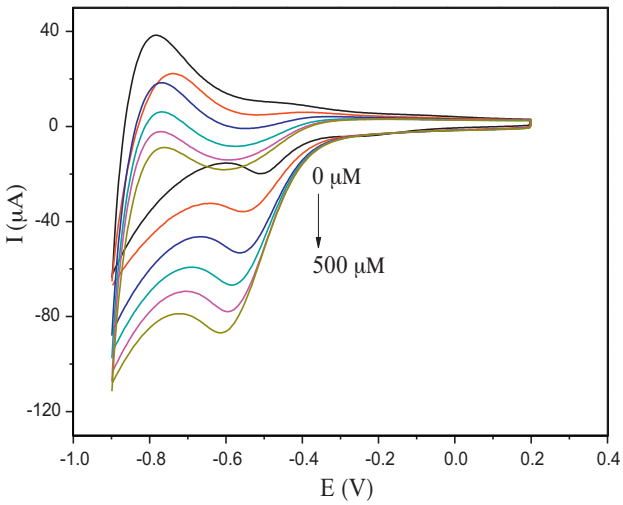

Fig. 5. CVs of Hb//3DOM GTD/ITO electrode with addition of different concentration of H_2O_2 in 0.1 M pH 7.0 PBS at a scan rate of 100 mV/s. [H_2O_2] = 0, 100, 200, 300, 400, 500 μM (from inner to outer).

nal surface but also on the internal surface of 3DOM structure. This result was also demonstrated by our previous study (Li et al., 2008). Comparing with the two strong reduction peaks, the two oxidation peaks were rather weak. This is attributed to the large band gap (3.2 eV) for this nanoporous material at higher potential (Topoglidis et al., 2001a,b). In addition, the reduction peak signal of the lower potential (reduction peak 1) was stronger than that of the higher potential (reduction peak 2). This might result from two reasons. One is the large band gap for this nanoporous material at higher potential. Another reason is Hb molecules immobilized on the internal surface more than that of the external surface of 3DOM structure. This 3DOM photonic crystals structure can provide 27 m^2/cm^3 internal surface area, which was remarkably larger than that of the external surface (Li and Zheng, 2008). This makes the reduction current (reduction peak 1) almost reach to 40 μA without the help of mediator molecules. These indicate that the direct electron transfer of Hb can be achieved on the 3DOM GTD/ITO electrode and our fabrication electrode is a good microenvironment for Hb immobilization.

3.3. Electrochemical properties of Hb/3DOM GTD/ITO electrode

Fig. 4 shows the cyclic measurements of the Hb/3DOM GTD/ITO electrode in PBS (pH 7.0) at various scan rates. The inset of Fig. 4 shows the linear dependence of the peak current on scan rate in the range from 20 to 300 mV s^{-1}, indicating that the electrochemical process of Hb at 3DOM GTD/ITO electrode was, as expected for an immobilized system, a surface-confined one. The peak to peak separations of the two couples of redox peak were 0.084 V and 0.193 V, respectively. The electron transfer rate constant k_s could be calculated according to the equation $k_s = mnF/RT$ when the peak-to peak separation was less than 200 mV (Laviron, 1979), where m is a parameter related to the peak-to-peak separation, n is the number of transfer electron. From Fig. 4 data, the k_s value was obtained to be 1.12 s^{-1}, which is higher than that of the Hb in the magnetic nanoparticles–chitosan film (1.04 s^{-1}) (Zheng et al., 2009), in the Au-colloid-cysteamine-modified gold electrode (0.49 s^{-1}) (Gu et al., 2001) and in the CNT powder microelectrodes (0.062 s^{-1}) (Zhao et al., 2005), indicating 3DOM GTD be benefit to the electron transfer of Hb.

The pH of the buffer solution affected the electrochemical behavior of Hb in the 3DOM GTD/ITO electrode. As shown in supplementary material Figure 2, the formal potential $E^{0'}$ depended linearly on the buffer pH, with a slope of −62.2 mV/pH (R = 0.9992), which is close to the expected value of −58.0 mV/pH for the one-proton transfer coupled one-electron-transfer reaction (Bond, 1980). Thus the electron-transfer between Hb and the electrode can be presented as following:

$$[\mathrm{HbFe(III)}] + e^- \leftrightarrow [\mathrm{HbFe(II)}] \quad (1)$$

3.4. Electrocatalytic reactivity of the immobilized Hb to H_2O_2

It is well known that proteins and enzymes containing the heme group, such as horseradish peroxidase, cytochrome c, hemoglobin and myoglobin, have the ability to reduce H_2O_2 electrocatalytically (Zheng et al., 2009). Fig. 5 shows CVs of the Hb/3DOM GTD/ITO electrode recorded in 0.1 M PBS at pH7.0 in the successive addition of 0.2 M H_2O_2 at 100 mV/s. With increasing H_2O_2 concentration, the reduction peak currents at −0.52 V increased significantly. However, the reduction peak currents of higher potential peak decreased and even disappeared in the high concentration of H_2O_2. This is attributed to the different formal potentials of the two couples of redox peak which are −0.48 and −0.20 V at the lower and higher potential, respectively (Fig. 3). The formal potential of Hb at the lower potential is close to that of native Hb in solution and the Hb at the lower potential is easy to be oxidized. In addition, no direct reduction peak was observed at Hb-free/3DOM GTD/ITO electrode in the presence of H_2O_2. Thus, the reduction peak current changes result from the reaction of Hb with H_2O_2. The electrocatalytic reaction can be expressed as following (Nassar et al., 1995b):

$$[\mathrm{HbFe(III)}] + e^- \leftrightarrow [\mathrm{HbFe(II)}]$$

$$2[\mathrm{HbFe(II)}] + H_2O_2 + 2H^+ + 2e^- \rightarrow 2[\mathrm{HbFe(III)}] + 2H_2O$$

Hb Fe(II) generated on the electrode was chemically oxidized by H_2O_2, and the produced Hb Fe(III) was reduced again at the electrode in a catalytic cycle. The oxidation rate of Hb Fe(II) by H_2O_2 was rather fast and the oxidation peaks disappeared in the higher concentration H_2O_2.

Fig. 6a shows the amperometric response of the Hb/3DOM GTD/ITO electrode to successive additions of H_2O_2 at potential −0.52 V in pH 7.0 PBS buffer. It exhibited a rapid and almost fifteen times current response to H_2O_2. We also compared the electrochemical response of Hb/GTDNs/ITO electrode with Hb/3DOM

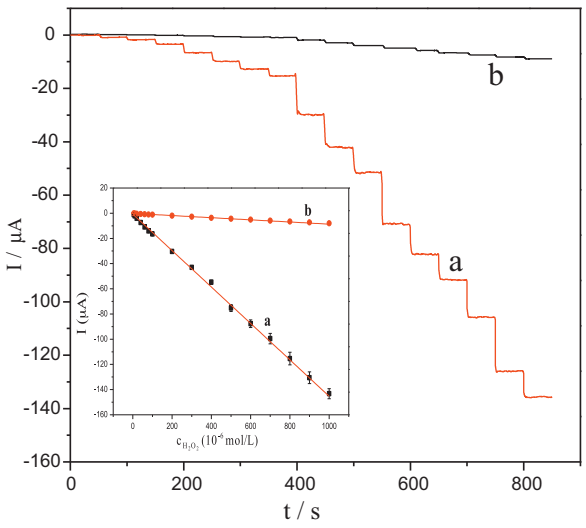

Fig. 6. Amperometric responses of Hb/3DOM GTD/ITO electrode (a) and Hb/GTDNs/ITO electrode (b) at an operating potential of −0.52 V upon successive additions of H_2O_2 in pH 7.0 PBS buffer. Inset shows the plot of catalytic current of Hb/3DOM GTD/ITO electrode (a) and Hb/GTDNs/ITO electrode (b) vs H_2O_2 concentration.

GTD/ITO electrode to H_2O_2 in pH 7.0 PBS solution. Fig. 6b shows the electrochemical response of Hb/GTDNs/ITO electrode under the same conditions of continuous addition of aliquot of H_2O_2 to the buffer solution. It can be seen that the Hb/GTDNs/ITO electrode yielded a detectable, but very small current response to H_2O_2. The inset of Fig. 6 exhibited the relationship between the reduction peak current of the Hb/3DOM GTD/ITO electrode and the H_2O_2 concentration. It showed that the reduction peak current values increased linearly with the concentration of H_2O_2 from 5.0 μM to 1.0 mM with a correlation coefficient of 0.9989 (n = 16). The limit of detection is 0.6 μM for a signal-to-noise ratio of 3, which was lower than 60 μM on a nickel oxide nanoparticles (Salimi et al., 2006), and 1.5 μM on a Hb/TiO_2 nanotube films (Liu et al., 2009).

Comparing the electrochemical response of Hb/GTDNs/ITO electrode with Hb/3DOM GTD/ITO electrode to H_2O_2 in pH 7.0 PBS solution, the Hb/3DOM GTD/ITO electrode has higher sensitivity and higher response peak current to the same concentration of H_2O_2. In the linear range, the Hb/3DOM GTD/ITO electrode has a high sensitivity of 144.5 μA mM^{-1}, which is higher than that of 8.53 μA mM^{-1} for Hb/GTDNs/ITO electrode. This was due to more Hb molecules immobilized on the surface of 3DOM structure than that of the GTDNs. The similar results were also reported in the studies of immobilized glucose on three-dimensional ordered macroporous prussian blue film (Qiu et al., 2007).

3.5. Stability and reproducibility of the Hb/3DOM GTD/ITO electrode

The stability of the sensor was evaluated by a lifetime experiment. The Hb/3DOM GTD/ITO electrode was stored in pH 7.0 PBS buffer at 4 °C and the response to 100 μM H_2O_2 was recorded periodically. The results showed that no obvious decrease in the response currents to H_2O_2 was observed after one month storage. The response currents to H_2O_2 decreased about 10% over a 50-day period, showing good storage stability. The CV currents of 100 μM H_2O_2 at the Hb/3DOM GTD/ITO electrode could remain 98% of the original signal after more than 50 successive cycles and the relative standard deviation (RSD) was below 5%. The electrode-to-electrode reproducibility was determined from the voltammetric signal for 100 μM H_2O_2 measured at three independent freshly prepared electrode, showing an acceptable reproducibility with a RSD of below 2%. The long-term stability and good reproducibility could be attributed to the fact that Hb molecules were strongly attached to the 3DOM GTD modified electrode surface.

4. Conclusions

We have developed a novel H_2O_2 biosensor based on the immobilization of Hb on the 3DOM GTD film. The immobilized Hb shows two couples of redox peaks assigning to the redox of Hb intercalated in the mesopores and adsorbed on the external surface of the mesoporous structure. The Hb/3DOM GTD/ITO biosensor exhibits a wide detection range, high sensitivity, long-term stability and acceptable reproducibility. The excellent catalytic activity and fast response to H_2O_2 are attributed to more reactive enzyme loading on the surface of 3DOM structure. The 3DOM GTD film is also used to immobilize other enzymes and other bioactive molecules and may find much more use in the fields of H_2O_2 biosensors.

Acknowledgements

This work was supported by the project of the Natural Science Foundation of China No.20833006.

Appendix A. Supplementary data

Supplementary data associated with this article can be found, in the online version, at doi:10.1016/j.bios.2011.02.010.

References

Armstrong, F.A., Wilson, G.S., 2000. Electrochim. Acta 45, 2623–2645.
Armstrong, F.A., Hill, H.A.O., Walton, N.J., 1988. Acc. Chem. Res. 21, 407–413.
Alwarappan, S., Liu, Kumar, A., Li, C.Z., 2010. J. Phys. Chem. C 114, 12920–12924.
Bartlett, P.N., Birkin, P.R., Wang, J.H., 1998. Anal. Chem. 70, 3685–3694.
Bing, Z., Yuan, Y., Wang, Y., Fu, Z.W., 2006. Electrochem. Solid-State Lett. 9, A101–A104.
Bond, A.M., 1980. Modern Polarographic Methods in Analytical Chemistry. CRC, New York, pp. 29–30.
Cao, H., Zhu, Y., Tang, L., Yang, X., Li, C., 2008a. Electroanalysis 20, 2223–2228.
Cao, W., Wei, C., Hu, J., Li, Q., 2008b. Electroanalysis 20, 1925–1931.
Chen, S.H., Yuan, R., Chai, Y.Q., Xu, L., Wang, N., Li, X.N., Zhang, L.Y., 2006. Electroanalysis 18, 471–477.
Dai, Z.H., Ju, H.X., Chen, H.Y., 2005. Electroanalysis 17, 862–868.
Doron, A., Katz, E., Willner, I., 1995. Langmuir 11, 1313–1317.
Environ, 2007. Sci. Technol. 41, 4405–4409.
Feng, J.J., Zhao, G., Xu, J.J., Chen, H.Y., 2005. Anal. Biochem. 342, 280–286.
Gu, H.Y., Yu, A.M., Chen, H.Y., 2001. J. Electroanal. Chem. 516, 119–126.
Hamachi, I., Fujita, A., Kunitake, T., 1997. J. Am. Chem. Soc. 119, 9096–9102.
Huisman, C.L., Schoonman, J., Goossens, A., 2005. Sol. Energy Mater. Sol. Cells 85, 115–124.
Laviron, E., 1979. J. Electroanal. Chem. 101, 19–28.
Li, J.L., Han, T., Wei, N.N., Du, J.Y., Zhao, X.W., 2009a. Biosens. Bioelectron. 25, 773–777.
Li, J.L., Zhao, X.W., Wei, H.M., Gu, Z.Z., Lu, Z.H., 2008. Anal. Chim. Acta 625, 63–69.
Li, J.L., Zheng, T.S., 2008. Sens. Actuators B131, 190–195.
Li, S.Q., Xia, J., Liu, C.Y., Zheng, Y.Z., Zeng, L., Hu, J.B., Li, Q.L., 2009b. Microchim. Acta 167, 41–46.
Liu, S.Q., Chen, A.C., 2005. Langmuir 21, 8409–8413.
Liu, M.C., Zhao, G.H., Zhao, K.J., Tong, X.L., Tang, Y.T., 2009. Electrochem. Commun. 11, 1397–1400.
Lu, L., Eychmueller, A., 2008. Acc. Chem. Res. 41, 244–253.
Ma, G.X., Lu, T.H., Xia, Y.Y., 2007. Bioelectrochemistry 71, 180–185.
Nassar, A.E.F., Willis, W.S., Rusling, J.F., 1995a. Anal. Chem. 67, 2386–2392.
Nassar, A.E.F., Zhang, Z., Chynwat, V., Frank, H.A., Rusling, J.F., Suga, K., 1995b. J. Phys. Chem. 99, 11013–11017.
Qiu, J.D., Peng, H.Z., Liang, R.P., Xiong, M., 2007. Electroanalysis 19, 1201–1206.
Song, Y.Y., Zhang, D., Gao, W., Xia, X.H., 2005. Chem. Eur. J. 11, 2177–2182.
Szamocki, R., Velichko, A., Holzapfel, C., Mucklich, F., Ravaine, S., Garrigue, P., Sojic, N., Hempelmann, R., Kuhn, A., 2007. Anal. Chem. 79, 533–539.
Szamocki, R., Reculusa, S., Ravaine, S., Bartlett, P.N., Kuhn, A., Hempelmann, R., 2006. Angew. Chem. Int. Ed. 45, 1317–1321.
Salimi, A., Sharifi, E., Noorbakhsh, A., Soltanian, S., 2006. Electrochem. Commun. 8, 1499–1508.
Szpakowska, M., Plocharska-Jankowska, E., Nagy, O.B., 2009. J. Phys. Chem. B 113, 15503–15512.
Tang, D.Y., Xia, B.Y., Zhang, Y.Q., 2008. Microchim. Acta 160, 367–374.
Teng, Y.J., Zuo, S.H., Lan, M.B., 2009. Biosens. Bioelectron. 24, 1353–1357.

Topoglidis, E., Campbell, C.J., Cass, A.E.G., Durrant, J.R., 2001a. Langmuir 17, 7899–7906.
Topoglidis, E., Cass, A.E.G., O'Regan, B., Durrant, J.R., 2001b. Electroanal. J. Chem. 517, 20–27.
You, J., Ding, W.P., Ding, S.J., Ju, H.X., 2009. Electroanalysis 21, 190–195.
Yu, J.H., Ju, H.X., 2003. Anal. Chim. Acta 486, 209–216.
Wei, W., Jin, H.H., Zhao, G.C., 2009. Microchim. Acta 164, 167–171.
Wu, Y.H., Hu, S.S., 2007. Microchim. Acta 159, 1–17.
Zhao, Y.D., Bi, Y.H., Zhang, W.D., Luo, Q.M., 2005. Talanta 65, 489–494.
Zhang, Y., He, P.L., Hu, N.F., 2004. Electrochim. Acta 49, 1981–1988.
Zheng, N., Zhou, X., Yang, W.Y., Li, X.J., Yuan, Z.B., 2009. Talanta 79, 780–786.
Zhu, Y.H., Cao, H.M., Tang, L.H., Yang, X.Y., Li, C.Z., 2009. Electrochim. Acta 54, 2823–2827.